Journal of Fluorine Chemistry 130 (2009) 248–253

Contents lists available at ScienceDirect

Journal of Fluorine Chemistry

journal homepage: www.elsevier.com/locate/fluor

Molecular association in 2-bromo-2-chloro-1,1,1-trifluoroethane (Halothane)

Anna Olejniczak [a], Andrzej Katrusiak [a,*], Pierangelo Metrangolo [b], Giuseppe Resnati [b]

[a] Faculty of Chemistry, Adam Mickiewicz University, Grunwaldzka 6, 60-780 Poznan, Poland
[b] Nanaostructured Fluorinated Materials Laboratory, DCMIC, Politecnico di Milano, 7, via Mancinelli, I-20131 Milano, Italy

ARTICLE INFO

Article history:
Received 23 September 2008
Received in revised form 29 October 2008
Accepted 30 October 2008
Available online 12 November 2008

Keywords:
Isochoric crystallization
Molecular disorder
Halogen···halogen interactions
Halogen···hydrogen interactions
High-pressure structure

ABSTRACT

Intermolecular interactions and the role of fluorine substitution have been investigated for a halogenated-ethane anesthetic. 2-Bromo-2-chloro-1,1,1-trifluoroethane, $BrClCHCF_3$ (Halothane), has been *in situ* pressure frozen in a diamond anvil cell and its structure determined by single-crystal X-ray diffraction at 1.85(5) GPa/296 K. Crystal is triclinic, space group $P\bar{1}$. In this racemic structure the enantiomorphic molecules are substitutionally disordered at the same general positions in that way that bromine and chlorine atoms occupy the same site at the 50:50 ratio. Despite the fact that only the Br and Cl atoms are disordered, the crystal packing is dominated by halogen···halogen and halogen···hydrogen interactions. This X-ray diffraction study provides structural explanation of considerably increased vapor pressure of Halothane compared to its hydrogenated analogue.

1. Introduction

Fluorinated compounds are of particular interest due to their unusual physical and chemical properties and a wide range of applications from medicine to modern technology materials [1]. The general anesthetics are mostly halogenated compounds. Halofluorocarbons are being used as inhalation anesthetics since mid of the twentieth century, the first anesthetic of this type, 2-bromo-2-chloro-1,1,1-trifluoroethane (Halothane), being introduced clinically in 1956. It has few undesired side-effects and the particular advantages of high chemical stability, high vapor pressure and non-flammability [1]. Medical applications of Halothane were intensively studied, but no structural studies were carried out. It is a liquid with low boiling point of 325 K [2] and only the energy minimization and *ab initio* calculations were performed to obtain the structure and properties the isolated molecule of this compound [3–9]. The theoretical studies on the intermolecular interactions and H-donor properties of Halothane and other anesthetics, and their ability to form complexes with other compounds were not conclusive—initially they suggested no H-donor properties for Halothane [3], whereas most recent results showed that weak hydrogen bonds involving the CH group can be formed [6–9].

The aim of this high-pressure X-ray diffraction study was to provide structural information on Halothane. We were particular interested in the type and role of intermolecular interactions for molecular association and crystal packing, and in their comparison with the structures of simple halogenated compounds containing no fluorine atoms [10]. This information is required for understanding increased vapor pressure of fluorinated compounds, which is advantageous for their applications as anesthetics. The bromine and chlorine atoms considerably differ in mass (79.90 u vs. 35.45 u), but their atomic radii (1.14 Å vs. 1.00 Å) and van der Waals radii (1.95 Å vs. 1.80 Å, respectively) [11] are similar. Thus it was intended to establish, if the differences between Br and Cl are sufficiently large for resolving their sites in the crystal structure, or if the position of Br and Cl atoms are disordered. Halothane molecules are chiral and the disorder of halogen atoms would reverse the handiness of the superimposed molecules.

2. Results and discussion

In all structures the presence of highly electronegative fluorine atoms considerably affects the charge distribution [12]. In Halothane the net atomic charges of the chlorine and bromine atoms increase compared to $BrClCHCH_3$, as illustrated in Fig. 1. The electrostatic potential on the surface of H atoms in $BrClCHCH_3$ is all positive, whereas on the surface of F atoms in $BrClCHCF_3$ is all negative.

In the crystal structure of Halothane the chlorine and bromine atoms are disordered and they occupy the common atomic sites with half occupancy for Br and Cl. The likely reasons for this kind of disorder are the small difference in van der Waals radii of Br and Cl atoms [11,13] and the similar charge distribution on their surface

* Corresponding author. Tel.: +48 61 8291443 fax: +48 61 8295015.
E-mail address: katran@amu.edu.pl (A. Katrusiak).

0022-1139/$ – see front matter © 2008 Elsevier B.V. All rights reserved.
doi:10.1016/j.jfluchem.2008.10.009

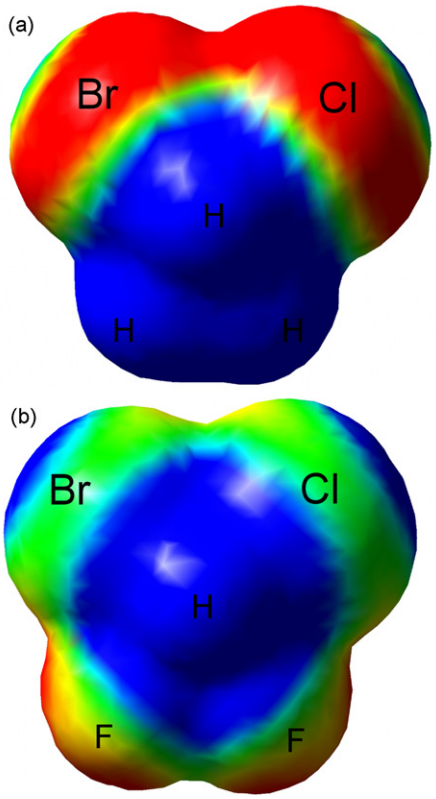

Fig. 1. Electrostatic potential indicated in the color scale, ranging from −1.0 (red) to 1.0 a.u. (blue), mapped onto the molecular surface of (a) $BrClCHCH_3$ and (b) $BrClCHCF_3$. (For interpretation of the references to color in this figure legend, the reader is referred to the web version of the article.)

(Fig. 1). Such a disorder is a frequent structural feature in compounds containing two different halogen atoms [14,15].

In Halothane the molecules lie in general positions and the molecular packing is governed by the contacts of bromine/chlorine atoms. The three shortest Br/Cl···Br/Cl, and the shortest Br/Cl···F and F···F arrange molecules along (1 1 0) planes. Within these planes the molecules are packed head to head over the inversion

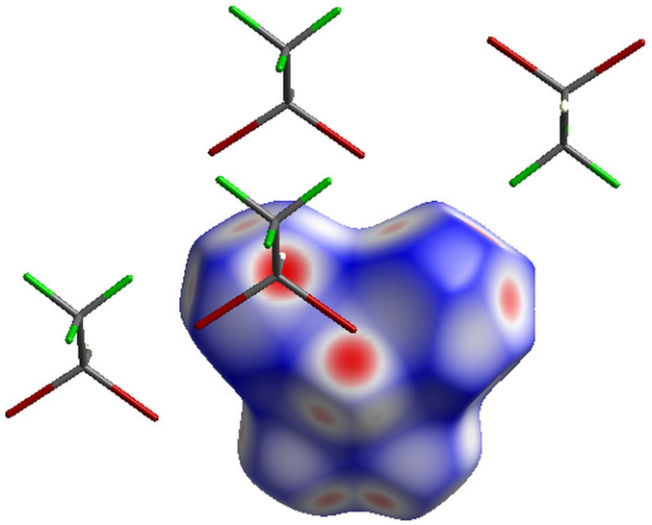

Fig. 3. Hirshfeld surfaces of Halothane molecule, decorated with the color scale depending on the distances of atoms to the surface points normalized relative to the atomic van der Waals radii. The surface points with intermolecular contacts closer than the sum of their van der Waals radii are highlighted in red, longer contacts are blue, and contacts around this sum are white. (For interpretation of the references to color in this figure legend, the reader is referred to the web version of the article.)

centre as shown in Fig. 2. The molecules of neighboring planes interact *via* short Br/Cl···H contacts. All the shortest intermolecular contacts are commensurate with sums of van der Waals radii [11]. The directions of intermolecular contacts involving halogen atoms and the distribution of electrostatic potential on the molecular surface suggest that the electrostatic contribution to the shortest Br/Cl···Br/Cl and F···F interactions is repulsive: the Br/Cl···Br/Cl and F···F angles have equal values on both sides of the contacts and the potentials in contact are equal in sign. According to this criterion, the electrostatic forces in the next shortest Br/Cl···Br/Cl and Br/Cl···H contacts are attractive. The substitution of H- by F-atoms introduces also a new type of Br/Cl···F interactions. The shortest of these interactions is attractive as it involves the positive regions of the Br/Cl atom. The intermolecular contacts of Halothane have been illustrated on its molecular Hirshfeld surface

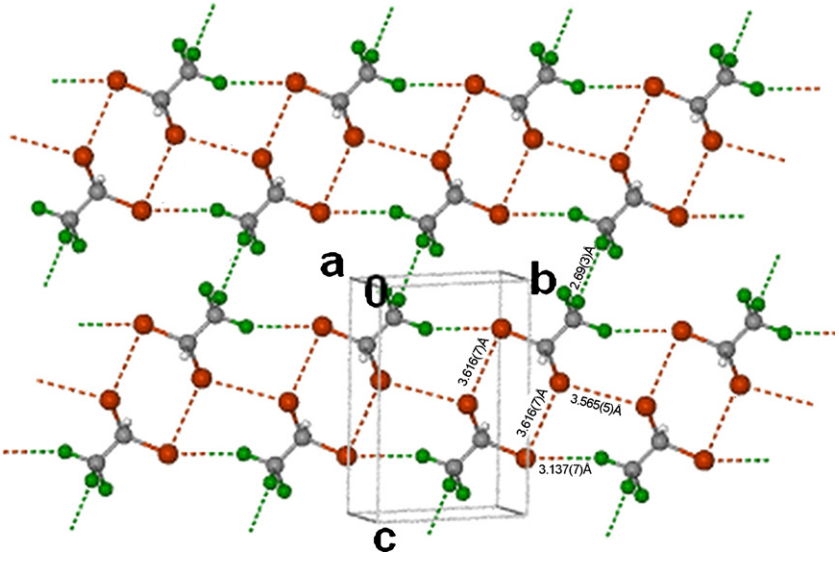

Fig. 2. A sheet arranged of molecules with the shortest Br/Cl···Br/Cl, Br/Cl···F and F···F contacts in the structure of $BrClCHCF_3$ at 1.85 GPa/296 K. The short contacts are indicated as dashed lines.

Table 1
The shortest contacts and relevant angles in the structure of Halothane and the weak CH···Br/Cl hydrogen bonds dimensions.

Distance [Å]		Angle [°]	
Br/Cl···Br/Cl^{i}	3.565(5)	C–Br/Cl···Br/Cl^{i}; Br/Cl···Br/Cl^{i}–C^{i}	103.2(4); 103.2(4)
Br/Cl···Br/Cl^{ii}	3.616(7)	C–Br/Cl···Br/Cl^{ii}; Br/Cl···Br/Cl^{ii}–C^{ii}	97(1); 142.1(4)
Br/Cl···Br/Cl^{ii}	3.616(7)	C–Br/Cl···Br/Cl^{ii}; Br/Cl···Br/Cl^{ii}–C^{ii}	142.1(4); 97(1)
C(H)···Br/Cl^{iii}	3.66(2)		
Br/Cl···H^{iii}	2.85(3)	C–Br/Cl···H^{iii}; Br/Cl···H^{iii}–C^{iii}	94.3(7); 138(1)
Br/Cl···F^{iv}	3.137(7)	C–Br/Cl···F^{iv}; Br/Cl···F^{iv}–C^{iv}	159(2); 156(1)
F···F^{v}	2.69(3)	C–F···F^{v}; F···F^{v}–C^{v}	147(2); 147(2)

Symmetry codes: (i) $-x, 3-y, 1-z$; (ii) $1-x, 2-y, 1-z$; (iii) $-x, 2-y, 1-z$; (iv) $x+1, y-1, z$; (v) $1-x, 3-y, -z$.

[16,17] in Fig. 3 and the shortest intermolecular distances are listed in Table 1.

The comparison of intermolecular interactions in the structures of $BrClCHCF_3$ and Cl_2CHCH_3 shows that the halogen···hydrogen contacts are only slightly shorter in $BrClCHCF_3$ and also there are F···F contacts shorter than sum of van der Waals radii whereas in Cl_2CHCH_3 no H···H contacts shorter than the sum of van der Waals radii are formed. However, the electrostatic potential on the surface of fluorine atoms in Halothane is negative and the overall negative-potential surface significantly increased in fluorinated molecules, and therefore the electrostatic repulsion between these negative regions can be considered as responsible for lower melting and boiling temperatures and higher vapor pressure of halogenated compounds.

Several types of disorder in the Halothane structure are possible. Fig. 4 shows possible configurations of molecules which form two neighboring centrosymmetric "dimers", as present in the crystal structure. The observed intermolecular Br/Cl···Br/Cl distances (Fig. 4, Table 1) are shorter than the sum of two van der Waals radii of Br atom (3.90 Å [11]), for all the clusters except RS:RS. The overlapped spheres for the other clusters (Fig. 4), indicate that the formation of RS dimers and RS:RS clusters are more favorable. This illustrates that the molecular disorder translational and orientational faults of mispositioned R and S enantiomers occurring at very short ranges introduce local strains in the Halothane structure. However, owing to the increased background associated with high-pressure X-ray diffraction experiments with a DAC, this type of disorder could not be evidenced by diffused scattering from the sample.

The energy Car-Parrinello minimization and molecular-dynamics simulations [3] led to the staggered conformation of Halothane molecule in the gas phase. The C–F bond staggered between the C–Br and C–Cl bonds is insignificantly shorter (by mere 0.007 Å) than the other C–F bonds. The molecular conformation determined in this study is very similar to that predicted theoretically. The calculated C–C and C–Cl bonds are typical for chloroalkans and other haloalkans, but in the solid state the Br and Cl-atom are disordered, and the C–Br/Cl bond length is average between those of C–Br and C–Cl [18]. The calculated valency angles in Halothane are slightly distorted from ideally tetrahedral values, similarly as in this crystal-structure result. That theoretical investigation [3] concluded that access to the H-atom in Halothane is hindered by adjacent voluminous halogens, and no evidence for CH···halogen bonding was found. More recent theoretical studies suggested that H-donor properties and formation of weak hydrogen bonds between Halothane and methanol, dimethyl ether, and in other complexes are possible [6–9]. In this study we found that the highly positive H-atom (Fig. 1) binds to the electronegative regions of the Br/Cl-atom, as inferred from the C-Br···H angle (Table 1). This illustrates the H-donor properties of the H-atom in Halothane and corroborates the theoretical results of the recent studies postulating the H-donor properties of Halothane

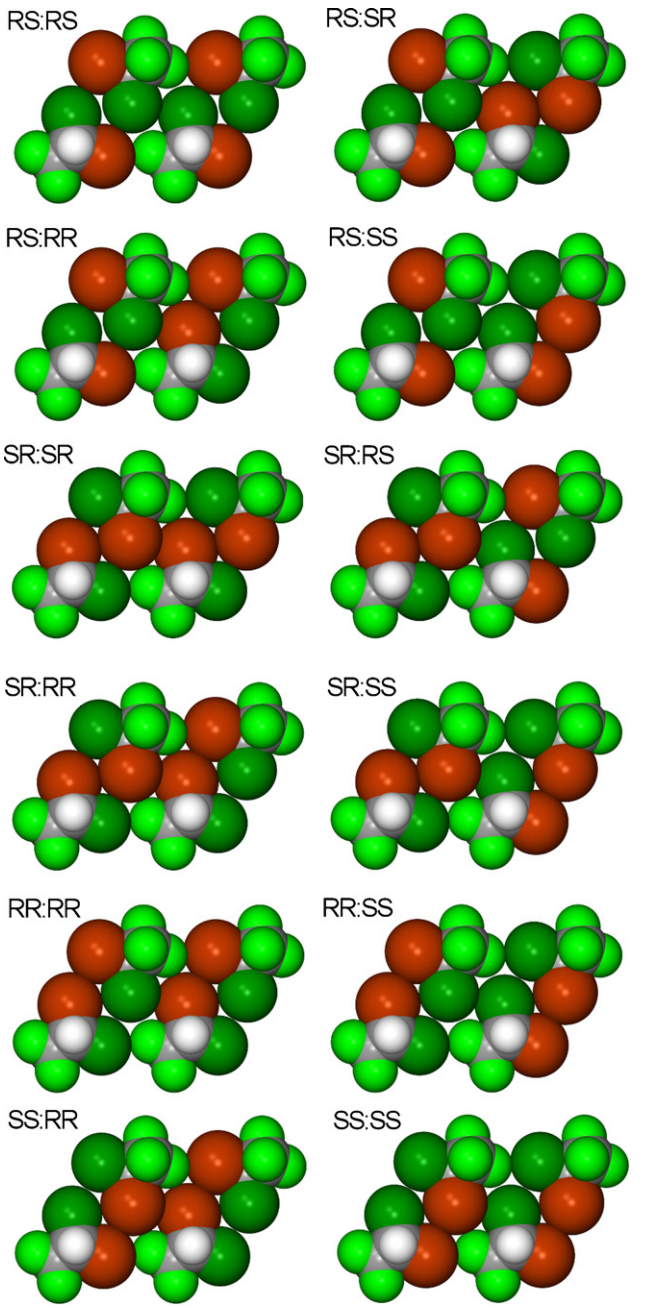

Fig. 4. The possible pairings of $BrClCHCF_3$ molecules forming dimers in crystal structure of Halothane. The molecules are represented by space-filling models: bromines dark red, chlorines dark green, fluorine light green. (For interpretation of the references to color in this figure legend, the reader is referred to the web version of the article.)

Table 2
Bond lengths [Å] and angles [°] for $BrClCHCF_3$. The dimensions involving not refined H-atoms in the X-ray data have been given without standard deviations.

	X-ray diffraction (this study)	DFT methods (staggered conformation) B3LYP/6-311G(2d,p)[a]
Br(1)–C(2)	1.858(18); 1.87(3)	1.957
Cl(1)–C(2)	1.858(18); 1.87(3)	1.779
F(3)–C(1)	1.31(2)	1.334
F(2)–C(1)	1.37(4)	1.343
F(1)–C(1)	1.32(2)	1.345
C(2)–C(1)	1.47(3)	1.533
C(1)–C(2)–Br(1)	111(2); 110(1)	110.6
C(1)–C(2)–Cl(1)	111(2); 110(1)	110.6
Br(1)–C(2)–Cl(1)	111.5(7); 111.5(7)	112.2
F(3)–C(1)–F(1)	107.7(9)	108.2
F(3)–C(1)–F(2)	105(1)	108.4
F(1)–C(1)–F(2)	105(3)	107.4
F(3)–C(1)–C(2)	114(3)	113.0
F(1)–C(1)–C(2)	114(1)	109.7
F(2)–C(1)–C(2)	111(1)	109.9
Br(1)–C(2)–C(1)–F(1)	176(1)	176.3
Cl(1)–C(2)–C(1)–F(1)	−60(1)	−58.7
Br(1)–C(2)–C(1)–F(2)	57(1)	58.4
Cl(1)–C(2)–C(1)–F(2)	−179(1)	−176.6
Br(1)–C(2)–C(1)–F(3)	−61(2)	−62.9
Cl(1)–C(2)–C(1)–F(3)	63(3)	62.1
H(1)–C(2)–C(1)–F(1)	56.85	59.8
H(1)–C(2)–C(1)–F(2)	−61.86	−58.1
H(1)–C(2)–C(1)–F(3)	−179.71	−179.4

[a] Ref. [5].

in its molecular complexes [6–9]. The structural dimensions of Halothane calculated theoretically [3–5,8] are consistent with these determined experimentally; also the molecular conformation and torsion angles calculated by Tang et al. [5] agree within errors with these in the crystal (Table 2).

3. Conclusions

We succeeded to obtain a single crystal of Halothane by isochoric freezing and to determine its crystal structure. The molecular arrangement in the Halothane crystal is predominantly governed by the close packing of molecules, while the electrostatic interactions of Br and Cl atoms are very weak. The structure investigated close to its melting curve is disordered, and the analysis of interactions and van der Waals radii suggests that this disorder is mainly due to the similar shape of the enantiomeric molecules in this crystal, where the molecular arrangement is governed by the close packing rule, and the intermolecular interactions are not discriminate between Br and Cl atoms. The electrostatic repulsion between the fluorine atoms is consistent with the lower melting and boiling points of Halothane and its higher vapor pressure compared to its hydrogenated analogues. Generally, weak interactions in molecular crystals are crucial for crystal packing and molecular aggregation, and are often responsible for the formation of polymorphs of organic compounds [19,20].

4. Experimental

4.1. General experimental procedures

Experiment was carried out using a miniature diamond-anvil cell (DAC) [21]. Pressure in the DAC was calibrated by ruby-fluorescence method [22,23], using a Betsa PRL spectrometer, with an accuracy of 0.05 GPa. The single-crystal X-ray diffraction measurement was carried out with a KUMA KM4-CCD diffractometer. The CrysAlis version 1.171.24 software [24] was used for the data collections [25] and the preliminary reduction of the data. The reflections intensities were corrected for the effects of DAC absorption, sample shadowing by the gasket, the sample absorption [26,27], and the sample reflections overlapping with diamond reflections have been eliminated. The Laue symmetry and intensities statistics suggested that the crystal is triclinic in space group $P\bar{1}$. The structure was solved straightforwardly by direct methods [28] and refined by full-matrix least-squares [29]. Anisotropic temperature factors were generally applied, but where the anisotropic refinement resulted in non-positive definite ellipsoids, isotropic thermal parameters were retained (for atoms C1, C2 and F2). The H-atom was located in a difference Fourier map and refined with $U_{iso} = 1.2U_{eq}$ of the C2. The isotropic refinement of the structure revealed that the Br and Cl atoms are disordered. To check the possibility of too high symmetry assignment it was attempted to refine the structure in the lower-symmetry space group $P1$, however it did not help to resolve the Br and Cl sites. It confirmed that the Br and Cl atoms are disordered in the centrosymmetric structure. The crystal data and the structure refinement details are listed in Table 3. Crystallographic data for the structure reported in this paper has been deposited with the Cambridge Crystallographic Data Centre as supplementary publication no. CCDC 685509. Structural drawings have been prepared with the X-Seed interface of POV-Ray [30,31]. The GAUSSIAN03 program suite and a PC were used for calculating the electrostatic potential on the molecular surface [32]. The calculations were carried out at the B3LYP/6-311G**(d,p) level of theory.

Table 3
Selected crystal data and details of structure refinement for $BrClCHCF_3$.

Empirical formula	$BrClCHCF_3$
Pressure (GPa)	1.85(5)
Temperature (K)	296(2)
Formula weight (g/mol)	197.39
Wavelength (Å)	Mo Kα 0.71073
Crystal system	Triclinic
Space group	$P\bar{1}$
Unit cell dimensions (Å,°)	$a = 4.4204(9)$ $b = 5.9854(12)$ $c = 9.0833(18)$ $\alpha = 88.25(3)$ $\beta = 80.69(3)$ $\gamma = 84.13(3)$
Volume (Å^3)	235.89(8)
Z	2
Calculated density (g/cm^3)	2.779
Absorption coefficient (mm^{-1})	9.204
$F(0\,0\,0)$	184
Crystal diameter/height (mm)	0.42/0.09
θ-range for data collection (°)	3.42–29.57
Min./max. indices h, k, l	−5/6, −8/8, −4/4
Reflect. collected/unique (R_{int})	1868/322 (0.0630)
Completeness (to θ_{max}) (%)	24.3 (to 29.57°)
Refinement method	Full-matrix least-squares on F^2
Data/restrains/parameters	322/3/53
Goodness-of-fit on F^2	1.137
Final R_1/wR_2 ($I > 2\sigma_1$)	0.0552/0.1265
R_1/wR_2 (all data)	0.0722/0.1483
Weighting scheme	$w = 1/(\mathrm{sigma}^2(F_o^2) + (0.0692P)^2 + 1.79P)$, where $P = (\mathrm{Max}(F_o^2, 0) + 2Fc^2)/3$
Largest diff. peak and hole (e Å^{-3})	0.440/−0.380

4.2. Crystallization of 2-bromo-2-chloro-1,1,1-trifluoroethane

Attempts to obtain single crystal of Halothane at isobaric conditions by lowering temperature failed, and we continued the crystallization at elevated pressure where simultaneous control of

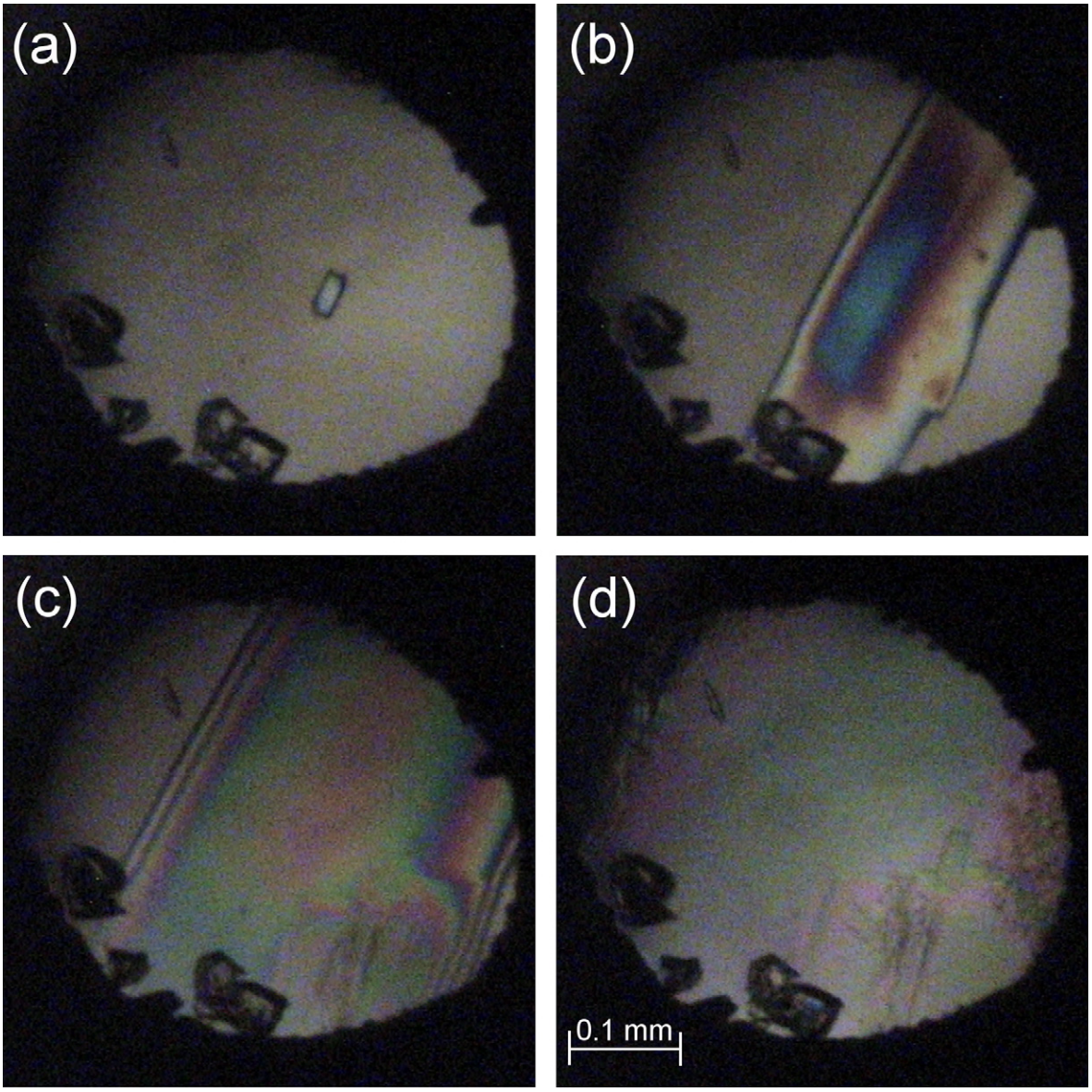

Fig. 5. Isochoric-growth stages of the Halothane single-crystal: (a) one small grain left of polycrystalline mass at 443 K; (b and c) the same crystal during slow temperature lowering between 440 and 433 K over 4 h and (d) the crystal filling whole volume of the DAC at 1.85 GPa/296 K. A few ruby chips for pressure calibration are grouped at the bottom-left edge of the DAC.

two thermodynamic parameters facilitates the growth of good quality crystals. Halothane was loaded into a diamond-anvil cell (DAC) [21] and pressure was increased slowly to 1.90 GPa, but the compound did not crystallize. Then the DAC was placed in solid CO_2 and when cooled to 210 K the liquid froze as a polycrystalline mass, which remained unchanged when warmed up to room temperature. In order to obtain a single crystal, the DAC was heated and all crystal grains but one melted, when the sample temperature increased to 443 K. By slowly lowering temperature this seed was grown at isochoric conditions into a single-crystal filling the whole chamber volume at 296 K (Fig. 5). The crystal first grew as an elongated thin plate, and after reaching the opposite sides it grew in the perpendicular directions to cover one diamond surface and finally it grew toward the other culet. The faces of the crystal were deformed and all the crystallization took about 9 h. The pressure calibration after one week gave 1.85 GPa. A diffraction measurement was carried out for this single crystal.

Acknowledgement

We are grateful to Dr. Ashwani Vij of the AFRL/RZSP, Edwards Air Force Base, California, for helpful discussions and encouragement.

References

[1] P. Kirsch, Modern Fluoroorganic Chemistry, Wiley-VCH, Weinheim, 2004.
[2] Sigma–Aldrich Corporation, Aldrich Advancing Science 2005–2006, Poland, 2005, p. 441.
[3] D. Scharf, K. Laasonen, Chem. Phys. Lett. 258 (1996) 276–282.
[4] F.J. Melendez, M.A. Palafox, J. Mol. Struct. Theochem. 493 (1999) 179–185.
[5] P. Tang, I. Zubrzycki, Y. Xu, J. Comput. Chem. 22 (2001) 436–444.
[6] Z. Liu, Y. Xu, A.C. Saladino, T. Wymore, P. Tang, J. Phys. Chem. A 108 (2004) 781–786.
[7] C. Sandorfy, J. Mol. Struct. 708 (2004) 3–5.
[8] B. Czarnik-Matusewicz, D. Michalska, C. Sandorfy, Th. Zeegers-Huyskens, Chem. Phys. 322 (2006) 331–342.
[9] B. Michielsen, W.A. Herrebout, B.J. van der Veken, ChemPhysChem 8 (2007) 1188–1198.

[10] M. Bujak, M. Podsiadło, A. Katrusiak, J. Phys. Chem. B112 (2008) 1184–1188.
[11] S.S. Batsanov, Inorg. Mater. 37 (2001) 1031–1046.
[12] P. Politzer, P. Lane, M.C. Concha, Y. Ma, J.S. Murray, J. Mol. Model. 13 (2007) 305–311.
[13] S.C. Nyburg, C.H. Faerman, Acta Crystallogr. B 41 (1985) 274–279.
[14] M. Podsiadło, A. Katrusiak, Acta Crystallogr. B 63 (2007) 903–911.
[15] Q. Huang, Z. Wang, Q. Chu, S. Zhu, J. Inclus. Phenom. Mol. Chem. 54 (2006) 177–180.
[16] J.J. McKinnon, M.A. Spackman, A.S. Mitchell, Acta Crystallogr. B60 (2004) 627–668.
[17] S.K. Wolff, D.J. Grimwood, J.J. McKinnon, D. Jayatilaka, M.A. Spackman, Crystal Explorer, Version 2.0, University of Western Australia, 2007.
[18] F.H. Allen, D.G. Watson, L. Brammer, A.G. Orpen, R. Taylor, in: E. Prince (Ed.), International Tables for Crystallography, vol. C, Kluwer Academic Publisher, Dordrecht, Boston, London, 2004 , p. 790 (Chapter 9.5).
[19] E.V. Boldyreva, Cryst. Eng. 6 (2003) 235–254.
[20] E.V. Boldyreva, S.N. Ivashevskaya, H. Sowa, H. Ahsbahs, H.-P. Weber, Z. Kristallogr. 220 (2005) 50–57.
[21] L. Merrill, W.A. Bassett, Rev. Sci. Instrum. 45 (1974) 290–294.
[22] G.J. Piermarini, S. Block, J.D. Barnett, R.A. Forman, J. Appl. Phys. 46 (1975) 2774–2780.
[23] H.K. Mao, J. Xu, P.M. Bell, J. Geophys. Res. 91 (1985) 4673–4676.
[24] Oxford Diffraction, CrysAlis CCD, Data collection GUI for CCD and CrysAlis RED CCD data reduction GUI, versions 1.171.24 beta, Wrocław, Poland, 2004.
[25] A. Budzianowski, A. Katrusiak, in: A. Katrusiak, P.F. McMillan (Eds.), High-Pressure Crystallography, vol. 140, Kluwer Academic Publisher, Dordrecht, 2004 , pp. 101–112 (Chapter 1).
[26] A. Katrusiak, REDSHABS. Program for the Correcting Reflections Intensities for DAC Absorption, Gasket Shadowing and Sample Crystal Absorption, Adam Mickiewicz University, Poznań, 2003.
[27] A. Katrusiak, Z. Kristallogr. 219 (2004) 461–467.
[28] G.M. Sheldrick, SHELXS97, University of Göttingen, Germany, 1997.
[29] G.M. Sheldrick, SHELXL97, University of Göttingen, Germany, 1997.
[30] L.J. Barbour, J. Supramol. Chem. 1 (2001) 189–191.
[31] Persistence of Vision Pty. Ltd., Williamstown, Victoria, Australia, Persistence of Vision (TM) Raytracer, Version 2.6, 2004.
[32] M.J. Frisch, et al., GAUSSIAN03, Revision B.04, Gaussian Inc., Pittsburgh, PA, 2003.